
<https://doi.org/10.15407/ujpe70.2.84>

S. CHATTOPADHYAY

Department of Mathematics, Sishu Bikash Academy
(Sonargaon, Teghoria, Narendrapur Station Road, P.O. – R.K.Pally,
P.S. – Narendrapur, Kolkata – 700150, West Bengal, India;
e-mail: sankardjln@gmail.com; ORCID No.: 0000-0003-4347-5762)

COMPARATIVE ANALYSIS OF DOUBLE LAYER PROFILES BETWEEN TWO-TEMPERATURE NON-ISOTHERMAL AND ISOTHERMAL ELECTRON PLASMAS

Double layers with a non-linear wave structure have been investigated by the well-known Sagdeev pseudopotential method in a plasma consisting of warm positive ions, warm negative ions, warm positrons, and two-temperature non-isothermal and isothermal electrons. In this work, the profiles of double layers from Sagdeev potential functions and double layer solutions for small-amplitude double layers between two-temperature non-isothermal and two-temperature isothermal electron plasmas are studied under a variation of the concentrations of positrons (χ), stream velocities of positive (u_{i0}) and negative (u_{j0}) ions, temperatures of positive (σ_i) and negative (σ_j) ions, and the concentration of negative ions (n_{j0}). The comparative studies of the small-amplitude double layers between two-temperature non-isothermal and two-temperature isothermal electron plasmas show the significant effect of the amplitudes and depth of the potential well. This comparative analysis of double-layer profiles between two-temperature non-isothermal and isothermal electron plasmas explores the differences in double-layer structures in plasma environments with distinct temperature profiles and provides valuable insights that can be applied across various domains in plasma physics.

Keywords: Sagdeev potential function, double layers, two-temperature non-isothermal and isothermal electrons, stream velocities, temperatures of positive and negative ions, concentrations of positrons and negative ions.

1. Introduction

Propagation of ion-acoustic solitary waves and double layers have been investigated by a large number of physicists [1–7] in a plasma comprising of warm adiabatic positive ions, warm adiabatic negative ions, warm isothermal positrons, and two-tempe-

rate non-isothermal or isothermal and non-thermal electrons through Sagdeev pseudopotential formalism in a magnetized or in an unmagnetized plasmas. In the past few years, besides solitons, many researchers had significant interest in double layers because of their relevance in cosmic applications [8], confinement of plasma in tandem mirror devices [9], and for ion heating in linear turbulence heating devices, *etc.*, [10]. Actually, ion-acoustic double layers have been found, when the soliton ends. Ion-acoustic double layers have also been observed in auroral [11] and magnetospheric [12] plasmas, where two-electron species exist. In the reductive perturbation method,

Citation: Chattopadhyay S. Comparative analysis of double layer profiles between two – temperature non-isothermal and isothermal electron. *Ukr. J. Phys.* **70**, No. 2, 84 (2025). <https://doi.org/10.15407/ujpe70.2.84>.

© Publisher PH “Akademperiodyka” of the NAS of Ukraine, 2025. This is an open access article under the CC BY-NC-ND license (<https://creativecommons.org/licenses/by-nc-nd/4.0/>)

the large- and small-amplitude ion-acoustic double layers in different plasma systems have been observed by several authors. The experimental observation of a strong double layer in a plasma consisting of positive ions, negative ions, and electrons had been reported by Merlino and Loomis [13]. On the other hand, several authors studied small-amplitude ion-acoustic double layers theoretically as well as experimentally in different plasmas by the reductive perturbation and Sagdeev pseudopotential [1] methods. Wong, Mamas, and Arnush [14] made use of SF₆, a gas of great electron affinity, in their experiment and obtained a negative ion plasma at a neutral gas pressure. Sato [15] also obtained a negative ion plasma containing K⁺ and SF₆⁻ ions, where electron fraction became very small. Mishra *et al.* [16] investigated very carefully the existence regions and the nature of the ion-acoustic double layers mentioning their amplitudes and widths for some realistic examples of plasmas containing the ion species (Ar⁺, SF₆⁻), (Ar⁺, F⁻), (H⁺, O₂⁻), and (H⁺, H⁻). In their investigation, they also showed that the presence of negative ion species drastically affects the existence regions and the nature of the ion-acoustic double layers. In two-electron Boltzmann model, Goswami *et al.* [17] studied the obliquely propagating double layers in a magnetic field. Using the reductive perturbation method, Gill *et al.* [18] investigated ion-acoustic solitons and double layers in non-thermal electrons with isothermal positive and negative ions. Chattopadhyay [19–21] also studied ion-acoustic compressive solitary waves of first and second orders in a single-temperature non-isothermal electron plasma for cold positive and negative ions and ion-acoustic compressive solitons and double layers in two-temperature non-isothermal electron plasma for warm positive and negative ions under a variation of different plasma parameters. Again, Mishra *et al.* [22] studied comprehensively the ion-acoustic solitons in a negative ion plasma with two-electron temperature distribution. In addition, Kumar *et al.* [23] investigated large-amplitude ion-acoustic solitons in a warm negative ion plasma with super thermal electrons. By following the conditions for the formation of double layers after a soliton structure, the present author also investigated small-amplitude ion-acoustic double layers [24] in a plasma containing warm positrons, warm negative ions, warm positive ions and two-temperature non-isothermal electrons

by the Sagdeev pseudopotential [1] method. It is now very interesting and important to carry on the comparative analysis of the profiles of double layers from Sagdeev potential functions and double-layer solutions between two-temperature non-isothermal and two-temperature isothermal electron plasmas under a variation of the concentration of positrons, concentration of negative ions, stream velocities of positive and negative ions, and temperatures of positive and negative ions. Actually, this comparative analysis explores the differences in double-layer structures in plasma environments with distinct temperature profiles. This study can help one to explain how double layers are formed in these environments and influence phenomena like auroras and solar flares.

The plan of the paper is organized in the following ways:

In Sec. 2, the set of normalized basic fluid equations for warm positive and negative ions along with the normalized concentration of two-temperature non-isothermal electrons, equation of state in the adiabatic case, concentration of positrons, boundary conditions, and charge neutrality conditions are taken. The concentration of two-temperature isothermal electrons are taken in Sec. 2.1. The Sagdeev potential functions $\psi(\phi)$ & $\psi_1(\phi)$ and double-layer solutions ϕ_{DL} & ϕ_{DL_1} for small-amplitude double layers in two-temperature non-isothermal and isothermal electron plasmas with proper boundary conditions can be observed in Secs. 2 and 2.1. Section 3 contains the results and discussions of the entire problem. The comparative studies of the Sagdeev potential functions [$\psi(\phi)$ & $\psi_1(\phi)$] and double-layer solutions [ϕ_{DL} & ϕ_{DL_1}] are shown in Sec. 4 for some chosen set of parameters consistent with the quasi-neutrality condition. Concluding remarks are given in Sec. 5.

2. Formulation: Two-Temperature Non-Isothermal Electron Plasma

We consider a collisionless, unmagnetized, non-relativistic plasma model consisting of warm adiabatic positive ions with temperature T_i and mass m_i , warm adiabatic negative ions with temperature T_j and mass m_j , warm isothermal positrons with temperature T_p and bi-Maxwellian two-temperature non-isothermal electrons with effective temperature T_{eff} and density n_e . We now wish to study, at first, the small-amplitude double layers for this bi-Maxwellian

lian two-temperature non-isothermal electron plasmas with warm ions and positrons. The bi-Maxwellian two-temperature non-isothermal electron distribution contains two groups of electrons, where one group is hotter than the another one. In this paper, we have taken trapped electron distribution because trapped electron distributions are crucial in plasma studies. They significantly influence plasma stability, wave-particle interactions, transport process, and the overall dynamical behavior of the system. In this context, it is important to mention that many Astrophysical and laboratory plasmas naturally consist of multiple species such as electrons, both positive and negative ions, and positrons. Each species may have different temperatures due to different energy distribution mechanisms which makes the plasma non-isothermal. Double layers can be formed in such plasmas due to differences in temperature and density among the charged species, leading to complex electrostatic potential structures. Consequently, this non-isothermal model is generally more accurate and representative of real plasma conditions. It allows for the greater flexibility in modeling the double-layer formation and can capture finer details of the process. If the goal is to simulate or understand double layers in natural or experimental plasmas more accurately, this approach would likely give better results. If the focus is on understanding basic mechanisms or if computational simplicity is desired, the isothermal model may be preferable.

Now, the set of normalized basic fluid equations appropriate to the low-frequency waves are

$$\frac{\partial n_\alpha}{\partial t} + \frac{\partial}{\partial x}(n_\alpha u_\alpha) = 0, \quad (1)$$

$$\frac{\partial u_\alpha}{\partial t} + u_\alpha \frac{\partial u_\alpha}{\partial x} + \frac{\sigma_\alpha}{Q_\alpha n_\alpha} \frac{\partial p_\alpha}{\partial x} = -\frac{Z_\alpha}{Q_\alpha} \frac{\partial \phi}{\partial x}, \quad (2)$$

$$\frac{\partial p_\alpha}{\partial t} + u_\alpha \frac{\partial p_\alpha}{\partial x} + 3p_\alpha \frac{\partial u_\alpha}{\partial x} = 0, \quad (3)$$

$$\frac{\partial^2 \phi}{\partial x^2} = n_e - \sum_\alpha Z_\alpha n_\alpha - n_p, \quad (4)$$

where $\alpha = i$ stands for positive ions, $\alpha = j$ stands for negative ions; n_α , n_e , n_p are the densities of positive (negative) ions, electrons, and positrons; u_α is the velocity of positive (negative) ions; σ_α is the temperature ratios of positive (negative) ions and electrons; p_α is the pressures of positive (negative) ions; Z_α is a charge of positive (negative) ions, $Z_\alpha = 1$ for $\alpha = i$

and $Z_\alpha = -Z$ for $\alpha = j$; Q_α is the mass ratio of negative (j) to positive (i) ions, $Q_\alpha = 1$ for $\alpha = i$ and $Q_\alpha = Q$ for $\alpha = j$.

Here, the electrons are assumed to be in quasi-equilibrium state with low-frequency ion-acoustic wave. We, thus, take the following general expression for the electron density [25–26] as

$$n_e(\phi) = \left(\int_{-\infty}^{-\sqrt{2\phi}} dv + \int_{\sqrt{2\phi}}^{\infty} dv \right) f + \frac{g_+}{2} [1 + \text{sgn}(\xi - \xi_m)] \int_{-\sqrt{2\phi}}^{\sqrt{2\phi}} dv f_+ + \frac{g_-}{2} [1 - \text{sgn}(\xi - \xi_m)] \int_{-\sqrt{2\phi}}^{\sqrt{2\phi}} dv f_-.$$

Here, the symbols f and f_\pm represent the free and the reflected electron distribution functions. The above mentioned density normalization constants g_+ and g_- are positive. In this case, electrons can have different densities depending on the sign of $(\xi - \xi_m)$, where ξ_m is the position of the minimum of ion-acoustic double-layer potential ($\phi = 0$) and $\text{sgn}(\xi - \xi_m)$ is the constant of motion for all the reflected particles.

By using the quasi-neutrality condition and the drift approximation for electrons in small-amplitude ion-acoustic double layers, we may expand the electron density $n_e(\phi)$ [25–27] as follows:

$$n_e(\phi) = 1 + A_1 \phi + \delta^{\frac{1}{2}} A_2 \text{sgn}(\xi - \xi_m) \phi^{\frac{3}{2}} + A_3 \phi^2 + \dots$$

The above co-efficients A_1 , A_2 , $A_3 \dots$ are given as:

$$\int_{-\infty}^{+\infty} dv f(v) = 1, \quad A_1 = -P \int dv \frac{1}{v} \frac{\partial f}{\partial v},$$

$$A_2 = \left(\frac{4\sqrt{2}}{3} \right) \{g_+ f_+''(0) + f_-''(0)\},$$

$$A_3 = -\frac{1}{2} P \int dv \left(\frac{1}{v} \frac{\partial}{\partial v} \right) f,$$

where P represents the principal value of the integral.

Again for general formulation of monotonic double layers, we now consider the following modified Schamel-type [25–29] electron distribution:

$$f = \frac{1}{\sqrt{2\pi}} \exp \left[-\frac{1}{2} (\text{sgn}(v)\sqrt{\varepsilon} - v_d)^2 \right] \theta(\varepsilon), \quad \varepsilon > 0,$$

$$f_{\pm} = \frac{1}{\sqrt{2\pi}} \exp\left(-\frac{1}{2} g_{\pm} v_d^2\right) \exp\left(-\frac{1}{2} \delta_{\pm} \varepsilon\right) \theta(-\varepsilon),$$

$$\varepsilon \leq 0.$$

Here, $\varepsilon^2 = v^2 - 2\phi$, $\phi(x) \geq 0$, and θ is a Heaviside step function.

The electron velocity and the potential are respectively normalized to the electron thermal velocity $\sqrt{\frac{K T_{\text{eff}}}{m_e}}$ and the electron temperature $\frac{K T_{\text{eff}}}{e}$, and v_d represents the electron drift velocity. The thermal distribution scaling (δ_{\pm}) are positive.

From the electron distribution functions given above, the corresponding density for electrons can be found by simple velocity-space integrations as follows:

$$n_e(\phi) = \exp\left(-\frac{v_d^2}{2}\right) \left[I\left(\frac{v_d^2}{2}, \phi\right) + T_{\pm}(\beta, \phi) \right].$$

Here, I and T are defined as follows:

$$I\left(\frac{v_d^2}{2}, \phi\right) = \sqrt{\frac{2}{\pi}} \times$$

$$\times \int_0^{\infty} dV \left[\frac{V}{\sqrt{V^2 + 2\phi}} \exp\left(-\frac{V^2}{2}\right) \cosh(V, v_d) \right],$$

$$T_+(\beta, \phi) = \frac{1}{\sqrt{\beta}} \exp(\beta\phi) \operatorname{erf}\left(\sqrt{\beta\phi}\right), \quad \beta > 0,$$

$$T_-(\beta, \phi) = \frac{2}{\sqrt{\pi}|\beta|} \exp(-|\beta|\phi) \int_0^{\sqrt{|\beta|\phi}} dy \exp(y^2),$$

$$\beta < 0.$$

Here, the ‘erf’ represents the error function.

In this paper, the electron density is defined from Vlasov equations consisting of free and trapped electrons as

$$n_e(\phi) = \int_{-\infty}^{\infty} f_e(x, v) dv =$$

$$= K_0 \left[\exp(\phi) \operatorname{erfc}\left(\sqrt{\phi}\right) + \frac{1}{\sqrt{\beta_1}} \times \right.$$

$$\left. \times \begin{cases} \exp(\beta_1\phi) \operatorname{erf}\left[\sqrt{|\beta_1\phi|}\right] & \text{for } \beta_1 \geq 0 \\ \frac{2}{\sqrt{\pi}} \exp\left[-\left\{\sqrt{|(-\beta_1\phi)|}\right\}^2\right] \times \\ \times \int_0^{\sqrt{|(-\beta_1\phi)|}} \exp(X^2) dX & \text{for } \beta_1 < 0 \end{cases} \right].$$

Here, $\operatorname{erf}(x) = \frac{2}{\sqrt{\pi}} \int_0^x e^{-t^2} dt$, $\operatorname{erfc}(x) = 1 - \operatorname{erf}(x)$, K_0 is some constant, and $f_e(x, v)$ is the electron distribution function with $\beta_1 = \frac{T_{el,f}}{T_{eh,t}}$ is the temperature ratio of free ($T_{el,f}$) and trapped ($T_{eh,t}$) electrons in low and high temperatures.

In the present paper, we consider the case $\beta_1 > 0$ and, thus, take

$$n_e(\phi) = \exp(\phi) \operatorname{erfc}\left(\sqrt{\phi}\right) + \frac{1}{\sqrt{\beta_1}} \exp(\beta_1\phi) \times$$

$$\times \operatorname{erf}\left[\sqrt{|\beta_1\phi|}\right] = \exp(\phi) \left[1 - \operatorname{erf}\left(\sqrt{\phi}\right) \right] +$$

$$+ \frac{1}{\sqrt{\beta_1}} \exp(\beta_1\phi) \operatorname{erf}\left[\sqrt{|\beta_1\phi|}\right] =$$

$$= \exp(\phi) \left[1 - \frac{2}{\sqrt{\pi}} \int_0^{\sqrt{\phi}} \exp(-t^2) dt \right] +$$

$$+ \frac{1}{\sqrt{\beta_1}} \exp(\beta_1\phi) \left[1 - \frac{2}{\sqrt{\pi}} \int_0^{\sqrt{\beta_1\phi}} \exp(-t^2) dt \right].$$

The normalized electron density $n_e(\phi)$ for two-temperature non-isothermal electron plasma is obtained by the Taylor series expansion from above under the condition $\phi \ll 1$ as

$$n_e = n_{el} + n_{eh} =$$

$$= \mu \left[1 + \left(\frac{\phi}{\mu + \nu\beta_1}\right) - \frac{4}{3} b_l \left(\frac{\phi}{\mu + \nu\beta_1}\right)^{\frac{3}{2}} + \right.$$

$$+ \frac{1}{2} \left(\frac{\phi}{\mu + \nu\beta_1}\right)^2 - \frac{8}{15} b_l^{(1)} \left(\frac{\phi}{\mu + \nu\beta_1}\right)^{\frac{5}{2}} +$$

$$+ \frac{1}{6} \left(\frac{\phi}{\mu + \nu\beta_1}\right)^3 + \dots \left. \right] + \nu \left[1 + \left(\frac{\beta_1\phi}{\mu + \nu\beta_1}\right) - \right.$$

$$- \frac{4}{3} b_h \left(\frac{\beta_1\phi}{\mu + \nu\beta_1}\right)^{\frac{3}{2}} + \frac{1}{2} \left(\frac{\beta_1\phi}{\mu + \nu\beta_1}\right)^2 -$$

$$- \frac{8}{15} b_h^{(1)} \left(\frac{\beta_1\phi}{\mu + \nu\beta_1}\right)^{\frac{5}{2}} + \frac{1}{6} \left(\frac{\beta_1\phi}{\mu + \nu\beta_1}\right)^3 + \dots \left. \right] =$$

$$= 1 + \phi - \frac{4}{3} \frac{(\mu b_l + \nu b_h \beta_1^{\frac{3}{2}})}{(\mu + \nu\beta_1)^{\frac{3}{2}}} \phi^{\frac{3}{2}} + \frac{1}{2} \frac{(\mu + \nu\beta_1^2)}{(\mu + \nu\beta_1)^2} \phi^2 -$$

$$- \frac{8}{15} \frac{(\mu b_l^{(1)} + \nu b_h^{(1)} \beta_1^{\frac{5}{2}})}{(\mu + \nu\beta_1)^{\frac{5}{2}}} \phi^{\frac{5}{2}} + \frac{1}{6} \frac{(\mu + \nu\beta_1^3)}{(\mu + \nu\beta_1)^3} \phi^3 - \dots, \quad (5)$$

where $0 < b_l$ or $b_h < \frac{1}{\sqrt{\pi}}$ and $0 < b_l^{(1)}$ or $b_h^{(1)} < \frac{1}{\sqrt{\pi}}$;
 $\beta_1 = \frac{T_{el,f}}{T_{eh,t}}$, $b_l = \frac{1-\beta_1}{\sqrt{\pi}}$, $b_h = \frac{1-\beta_h}{\sqrt{\pi}}$, $b_l^{(1)} = \frac{1-\beta_l^2}{\sqrt{\pi}}$, $b_h^{(1)} =$

$$= \frac{1-\beta_h^2}{\sqrt{\pi}}, \beta_l = \frac{T_{el,f}}{T_{el,t}}, \beta_h = \frac{T_{eh,f}}{T_{eh,t}}, \mu + \nu = 1, \sigma_\alpha = \frac{T_\alpha}{T_{\text{eff}}},$$

$$Q = \left(\frac{m_i}{m_e}\right)^{\frac{1}{2}} [i \text{ is for positive ion, } j \text{ is for negative ion}],$$

$$T_{\text{eff}} = \frac{T_{el} T_{eh}}{\mu T_{eh} + \nu T_{el}}, \mu \text{ and } \nu \text{ are unperturbed number density of low- temperature and high-temperature electrons; } T_{el,f} \text{ \& } T_{el,t} \text{ are the temperatures of free and trapped electrons in low temperatures, whereas } T_{eh,f} \text{ \& } T_{eh,t} \text{ are the temperatures of free and trapped electrons in high temperatures.}$$

Consequently in our present problem, untrapped ions and untrapped positrons are typically considered in such studies to simplify the model, focus on the electron-driven dynamics of double-layer formation and ensure analytical and numerical tractability. The behavior of trapped ions and positrons may add unnecessary complexity to the study without providing significant additional insights into the primary objective of comparing double-layer profiles in plasmas with different electron distributions. To avoid the complexity of taking trapped ions and positrons, we consider our present plasma model.

The normalized positron density (n_p) is

$$n_p = \chi e^{-\sigma_p \phi}, \quad (6)$$

where $\sigma_p = \frac{T_{\text{eff}}}{T_p}$ is the temperature ratios of effective electrons (T_{eff}) and positrons (T_p).

The charge neutrality condition is

$$1 + Zn_{j0} = n_{i0} + \chi \quad (7)$$

and the boundary conditions are

$$\begin{aligned} n_\alpha &\rightarrow n_{\alpha 0}, \quad u_\alpha \rightarrow u_{\alpha 0}, \quad p_\alpha \rightarrow p_{\alpha 0}, \quad n_e \rightarrow 1, \\ n_p &\rightarrow \chi \quad \text{and} \quad \phi \rightarrow 0 \quad \text{at} \quad |x| \rightarrow \infty. \end{aligned} \quad (8)$$

The equations (1) to (6) are normalized by the following ways:

Densities n_α , n_e and n_p are normalized by their equilibrium values n_0 ; velocities u_α by the ion-acoustic wave speed $C_s = \sqrt{\frac{KT_{\text{eff}}}{m_\alpha}}$, where m_α is the mass of ions, T_{eff} is the effective temperature of electrons, and K is the Boltzmann constant; pressures p_α by $p_0 = Kn_0T_\alpha$, where T_α is the temperature of ions; potential (ϕ) by $\frac{KeT_{\text{eff}}}{e}$, where e is the electron charge; time (t) by the inverse of the ion-plasma frequency in the mixture $\omega_{p_\alpha}^{-1} = \sqrt{\frac{m_\alpha}{4\pi n_0 e^2}}$ and the space co-ordinate (x) by the Debye length $\lambda_D = \sqrt{\frac{KT_{\text{eff}}}{4\pi n_0 e^2}}$

where $\alpha = i$ stands for positive ions, and $\alpha = j$ stands for negative ions.

Now, by using the Galelian transformation $\eta = x - Vt$, where V is the velocity of the solitary waves, we get, from Eqs. (1), to (4) as

$$-V \frac{\partial n_\alpha}{\partial \eta} + \frac{\partial}{\partial \eta}(n_\alpha u_\alpha) = 0, \quad (9)$$

$$-V \frac{\partial u_\alpha}{\partial \eta} + u_\alpha \frac{\partial u_\alpha}{\partial \eta} + \frac{\sigma_\alpha}{Q_\alpha n_\alpha} \frac{\partial p_\alpha}{\partial \eta} = -\frac{Z_\alpha}{Q_\alpha} \frac{\partial \phi}{\partial \eta}, \quad (10)$$

$$-V \frac{\partial p_\alpha}{\partial \eta} + u_\alpha \frac{\partial p_\alpha}{\partial \eta} + 3p_\alpha \frac{\partial u_\alpha}{\partial \eta} = 0, \quad (11)$$

$$\frac{\partial^2 \phi}{\partial \eta^2} = n_e - \sum_\alpha Z_\alpha n_\alpha - n_p. \quad (12)$$

As we consider the adiabatic case, Eq. (11) for positive and negative ions are consistent with the equations of state

$$p_\alpha = p_{\alpha 0} \left(\frac{n_\alpha}{n_{\alpha 0}}\right)^3 \quad (13)$$

and, hence, we shall take $p_{\alpha 0} = 1$.

From Eqs. (9), (10) & (12) after using the boundary conditions (8) and the equations of state (13), we get finally the Sagdeev potential function $\psi(\phi)$ by the non-perturbative or Sagdeev potential [1] approach as

$$\begin{aligned} \psi(\phi) = & \left[-\phi - \frac{1}{2}\phi^2 + \frac{8}{15} \frac{\mu b_l + \nu b_h \beta_1^{\frac{3}{2}}}{(\mu + \nu \beta_1)^{\frac{3}{2}}} \phi^{\frac{5}{2}} - \right. \\ & - \frac{1}{6} \frac{\mu + \nu \beta_1^2}{(\mu + \nu \beta_1)^2} \phi^3 + \frac{16}{105} \frac{\mu b_l^{(1)} + \nu b_h^{(1)} \beta_1^{\frac{5}{2}}}{(\mu + \nu \beta_1)^{\frac{5}{2}}} \phi^{\frac{7}{2}} - \\ & \left. - \frac{1}{24} \frac{\mu + \nu \beta_1^3}{(\mu + \nu \beta_1)^3} \phi^4 + \dots \right] + \\ & + \frac{1}{6} \sum_\alpha \sqrt{\frac{Q_\alpha^3 n_{\alpha 0}^3}{3 \sigma_\alpha}} \left[\left\{ \left(V - u_{\alpha 0} - \sqrt{\frac{3 \sigma_\alpha}{Q_\alpha n_{\alpha 0}}} \right)^2 - \right. \right. \\ & \left. \left. - \frac{2 Z_\alpha}{Q_\alpha} \phi \right\}^{\frac{3}{2}} - \left\{ \left(V - u_{\alpha 0} + \sqrt{\frac{3 \sigma_\alpha}{Q_\alpha n_{\alpha 0}}} \right)^2 - \frac{2 Z_\alpha}{Q_\alpha} \phi \right\}^{\frac{3}{2}} \right] \\ & + \left(V - u_{\alpha 0} + \sqrt{\frac{3 \sigma_\alpha}{Q_\alpha n_{\alpha 0}}} \right)^3 - \\ & - \left(V - u_{\alpha 0} - \sqrt{\frac{3 \sigma_\alpha}{Q_\alpha n_{\alpha 0}}} \right)^3 \left. \right] + \frac{\chi}{\sigma_p} (1 - e^{-\sigma_p \phi}), \quad (14) \end{aligned}$$

where

$$n_\alpha = \sum_\alpha \sqrt{\frac{Q_\alpha n_{\alpha 0}^3}{12 \sigma_\alpha}} \left[\left\{ \left(V - u_{\alpha 0} + \sqrt{\frac{3 \sigma_\alpha}{Q_\alpha n_{\alpha 0}}} \right)^2 - \frac{2 Z_\alpha}{Q_\alpha} \phi \right\}^{\frac{1}{2}} - \left\{ \left(V - u_{\alpha 0} - \sqrt{\frac{3 \sigma_\alpha}{Q_\alpha n_{\alpha 0}}} \right)^2 - \frac{2 Z_\alpha}{Q_\alpha} \phi \right\}^{\frac{1}{2}} \right]. \quad (15)$$

The restriction on ϕ is

$$-\frac{Q}{2Z} \left(V - u_{j0} - \sqrt{\frac{3 \sigma_j}{Q n_{j0}}} \right)^2 < \Phi < \frac{1}{2} \left(V - u_{i0} - \sqrt{\frac{3 \sigma_i}{n_{i0}}} \right)^2.$$

Expanding $\psi(\phi)$ in power of ϕ by the Taylor series expansion, we get, from equation (12),

$$\frac{d^2 \phi}{d\eta^2} = G_1 \phi - G_2 \phi^{\frac{3}{2}} + G_3 \phi^2 - G_4 \phi^{\frac{5}{2}} + G_5 \phi^3 - \dots = -\frac{\partial \psi}{\partial \phi} \quad (16)$$

and

$$\psi(\phi) = -\frac{1}{2} G_1 \phi^2 + \frac{2}{5} G_2 \phi^{\frac{5}{2}} - \frac{1}{3} G_3 \phi^3 + \frac{2}{7} G_4 \phi^{\frac{7}{2}} - \frac{1}{4} G_5 \phi^4, \quad (17)$$

where

$$G_1 = \left[1 - n_{i0} \left\{ (V - u_{i0})^2 - \frac{3 \sigma_i}{n_{i0}} \right\}^{-1} - Z^2 n_{j0} \left\{ Q (V - u_{j0})^2 - \frac{3 \sigma_j}{n_{j0}} \right\}^{-1} + \chi \sigma_p \right],$$

$$G_2 = \frac{4}{3} \frac{(\mu b_l + \nu b_h \beta_1^{\frac{3}{2}})}{(\mu + \nu \beta_1)^{\frac{3}{2}}},$$

$$G_3 = \frac{1}{2} \left[\frac{\mu + \nu \beta_1^2}{(\mu + \nu \beta_1)^2} - \frac{n_{i0}^{\frac{3}{2}}}{2 \sqrt{3 \sigma_i}} \left\{ \left(V - u_{i0} - \sqrt{\frac{3 \sigma_i}{n_{i0}}} \right)^{-3} - \left(V - u_{i0} + \sqrt{\frac{3 \sigma_i}{n_{i0}}} \right)^{-3} \right\} + \frac{Z^3 n_{j0}^{\frac{3}{2}}}{2 Q \sqrt{3 Q \sigma_j}} \left\{ \left(V - u_{j0} - \sqrt{\frac{3 \sigma_j}{Q n_{j0}}} \right)^{-3} - \left(V - u_{j0} + \sqrt{\frac{3 \sigma_j}{Q n_{j0}}} \right)^{-3} \right\} - \chi \sigma_p^2 \right],$$

$$G_4 = \frac{8}{15} \frac{(\mu b_l^{(1)} + \nu b_h^{(1)} \beta_1^{\frac{5}{2}})}{(\mu + \nu \beta_1)^{\frac{5}{2}}},$$

$$G_5 = \frac{1}{2} \left[\frac{1}{3} \frac{\mu + \nu \beta_1^3}{(\mu + \nu \beta_1)^3} - \frac{n_{i0}^{\frac{3}{2}}}{2 \sqrt{3 \sigma_i}} \left\{ \left(V - u_{i0} - \sqrt{\frac{3 \sigma_i}{n_{i0}}} \right)^{-5} - \left(V - u_{i0} + \sqrt{\frac{3 \sigma_i}{n_{i0}}} \right)^{-5} \right\} + \frac{Z^4 n_{j0}^{\frac{3}{2}}}{2 Q^2 \sqrt{3 \sigma_j Q}} \left\{ \left(V - u_{j0} - \sqrt{\frac{3 \sigma_j}{Q n_{j0}}} \right)^{-5} - \left(V - u_{j0} + \sqrt{\frac{3 \sigma_j}{Q n_{j0}}} \right)^{-5} \right\} + \frac{\chi \sigma_p^3}{3} \right]. \quad (18)$$

The formation of double layers may be observed by the following conditions:

- (i) $\psi(\phi) = 0$ at $\phi = 0$ and $\phi = \phi_m$,
- (ii) $\frac{\partial \psi}{\partial \phi} = 0$ at $\phi = 0$ and $\phi = \phi_m$,
- (iii) $\frac{\partial^2 \psi}{\partial \phi^2} < 0$ at $\phi = 0$ and $\phi = \phi_m$,
- (iv) $\psi(\phi) < 0$ for $0 < \phi < \phi_m$ and $\phi > \phi_m$.

For small-amplitude double layers, taking terms up to ϕ^2 from (16) and terms up to ϕ^3 from (17), we get

$$\frac{d^2 \phi}{d\eta^2} = -\frac{\partial \psi}{\partial \phi} = G_1 \phi - G_2 \phi^{\frac{3}{2}} + G_3 \phi^2, \quad (20)$$

$$\psi(\phi) = -\frac{1}{2} G_1 \phi^2 + \frac{2}{5} G_2 \phi^{\frac{5}{2}} - \frac{1}{3} G_3 \phi^3. \quad (21)$$

Using the above boundary conditions (19) for Eqs. (20) and (21) for double layers, we obtain the following relations for small-amplitude double layers in two-temperature non-isothermal electron plasmas:

$$G_1 = \frac{2}{3} G_3 \phi_m \quad \text{and} \quad G_2 = \frac{5}{3} G_3 \phi_m^{\frac{1}{2}},$$

$$\psi(\phi) = -\frac{1}{3} G_3 \phi^2 (\sqrt{\phi} - \sqrt{\phi_m})^2,$$

$$\frac{\partial \psi(\phi)}{\partial \phi} = -\frac{1}{3} G_3 \phi (\sqrt{\phi} - \sqrt{\phi_m}) (3 \sqrt{\phi} - 2 \sqrt{\phi_m}), \quad (22)$$

$$\phi_{DL} = \frac{1}{4} \phi_m \left[1 - \tanh \left(\sqrt{\frac{G_3 \phi_m}{24}} \eta \right) \right]^2,$$

where $G_3 > 0$.

The profiles of the Sagdeev potential function $\psi(\phi)$ against ϕ and double-layer solutions ϕ_{DL} against η for small-amplitude double layers in two-temperature non-isothermal electron plasmas may be drawn under a variation of the concentration of positrons (χ), stream velocities of positive (u_{i0}) and negative (u_{j0}) ions, temperatures of positive (σ_i) and negative (σ_j) ions, and the concentrations of negative (n_{j0}) ions.

2.1. Two-temperature Isothermal electron plasma

Now, we discuss the small-amplitude double layers for bi-Maxwellian two-temperature isothermal electron plasmas.

In this case, the previous normalized fluid equations (1) to (4) and the relations (6) to (8) will remain as the same for this two-temperature isothermal electron plasmas.

For bi-Maxwellian two-temperature isothermal electron plasmas, the normalized concentration of electrons will be

$$n_e = \mu \exp\left(\frac{\phi}{\mu + \nu\beta_1}\right) + \nu \exp\left(\frac{\beta_1\phi}{\mu + \nu\beta_1}\right), \quad (23)$$

where $\beta_1 = \frac{T_{el,f}}{T_{eh,t}}$ is the temperature ratio of free electrons in low and high temperatures, and μ, ν are the same as before. The normalization is done here by the previous mentioned ways. Using the transformation $\eta = x - Vt$ and the boundary conditions (8), we get finally, from Eqs. (1) to (4), (6) to (7), and (23) as

$$\frac{d^2\phi}{d\eta^2} = G_1\phi + G_3\phi^2 + G_5\phi^3 = -\frac{\partial\psi_1}{\partial\phi} \quad (24)$$

and

$$\psi_1(\phi) = -\frac{1}{2}G_1\phi^2 - \frac{1}{3}G_3\phi^3 - \frac{1}{4}G_5\phi^4, \quad (25)$$

where G_1, G_3 & G_5 are same for both two-temperature non-isothermal and two-temperature isothermal electron plasmas, and $\psi_1(\phi)$ is the Sagdeev potential function for two-temperature isothermal electron plasmas. Here, the boundary conditions for double layers are

$$\begin{aligned} \psi_1(\phi) &= 0 \quad \text{for} \quad \phi = 0 \quad \text{and} \quad \phi_{m_1}, \\ \frac{\partial\psi_1(\phi)}{\partial\phi} &= 0 \quad \text{for} \quad \phi = 0 \quad \text{and} \quad \phi_{m_1}. \end{aligned}$$

After using the boundary conditions for small-amplitude double layers for Eqs. (24) & (25), we get finally,

$$G_1 = \frac{1}{2}G_5\phi_{m_1}^2 \quad \text{and} \quad G_3 = -\frac{3}{2}G_5\phi_{m_1}.$$

Putting G_1 and G_3 in Eqs. (25) and (24), we get

$$\psi_1(\phi) = -\frac{1}{4}G_5\phi^2(\phi - \phi_{m_1})^2,$$

$$\frac{\partial\psi_1(\phi)}{\partial\phi} = -\frac{1}{2}G_5\phi(\phi - \phi_{m_1})(2\phi - \phi_{m_1})$$

and

$$\phi_{DL_1} = \frac{1}{2}\phi_{m_1} \left[1 - \tanh\left(\sqrt{\frac{G_5\phi_{m_1}}{8}}\eta\right) \right], \quad (26)$$

where ϕ_{m_1} is the maximum (minimum) value of ϕ at which double layer conditions are satisfied for two-temperature isothermal electron plasmas. The double layers can exist only when $G_5 > 0$. The physical existence of the double layers in a two-temperature isothermal electron plasma is thus purely governed by the value of G_5 .

3. Results and Discussions

In this section, we will draw the profiles of the double layers from Sagdeev potential functions $\psi(\phi)$ & $\psi_1(\phi)$ against ϕ and double-layer solutions ϕ_{DL} and ϕ_{DL_1} against η for small-amplitude double layers. Finally, we have also compared those double-layer profiles between two-temperature non-isothermal and isothermal electron plasmas under variations of some plasma parameters. The choice of parameters in the study of double layers in two-temperature non-isothermal and isothermal electron plasmas is guided by the specific physical conditions for the system under investigation. The goal is to create conditions where double layers can be formed, stabilized and be studied, whether in theoretical simulations [30–32] or experimental [33–35] settings. Actually, the parameters are chosen to reflect the realistic plasma conditions, to test hypotheses, or to match experimental constraints. Indeed, the roles of the soliton velocity V and the concentration (χ) of positrons for the formation of double layers in both two-temperature non-isothermal and isothermal electron plasmas are very much important and attractive. In most cases,

the values of V at which double layers occur in two-temperature non-isothermal and isothermal electron plasmas are different. But, in some simplified or idealized models for comparison of double layers, we take some specific values or same values of V at which double layer occurs and satisfies the necessary boundary conditions of the double layers. Moreover, the concentration (χ) of positrons lies in the range $0 \leq \chi < 1$ at which small-amplitude double layers occur in both two-temperature non-isothermal and isothermal electron plasmas maintaining the charge neutrality condition.

In Fig. 1, the profiles of the double layers from Sagdeev potential functions $\psi(\phi)$ & $\psi_1(\phi)$ against ϕ for small-amplitude double layers are compared between two-temperature non-isothermal [$\psi(\phi)$] & isothermal [$\psi_1(\phi)$] electron plasmas under the variation of the concentrations of positrons (χ). In our model, the double layers are found at a particular value of V with all other connected parameters after the ends of solitons. Actually, the double layer starts with upper limits of soliton velocity V , when soliton ends with some velocity of V . The Sagdeev potential functions $\psi(\phi)$ for two-temperature non-isothermal electron plasmas are denoted by a_1 for $\chi = 0.12$ and a_2 for $\chi = 0.17$ whereas the Sagdeev potential functions $\psi_1(\phi)$ for two-temperature isothermal electron plasmas are denoted by b_1 for $\chi = 0.12$ and b_2 for $\chi = 0.17$. It is evident from this figure that the amplitudes of the Sagdeev potential functions $\psi(\phi)$ for two-temperature non-isothermal electron plasmas are larger than the amplitudes of the Sagdeev potential functions $\psi_1(\phi)$ for two-temperature isothermal electron plasmas. Moreover the depth of the well for two-temperature isothermal electron plasma is higher than that of two-temperature non-isothermal electron plasma in our model.

Figure 2 shows the profiles of the double-layer solutions ϕ_{DL} and ϕ_{DL_1} against η for small-amplitude double layers between two-temperature non-isothermal & isothermal electron plasmas under the variation of the concentration of positrons (χ). The double-layer solutions ϕ_{DL} for two-temperature non-isothermal electron plasmas are denoted by a_3 for $\chi = 0.12$ and a_4 for $\chi = 0.17$ whereas the double-layer solutions ϕ_{DL_1} for two-temperature isothermal electron plasmas are denoted by b_3 for $\chi = 0.12$ and b_4 for $\chi = 0.17$. From this figure, among the curves a_3, a_4, b_3 and b_4 , it is seen that the curves

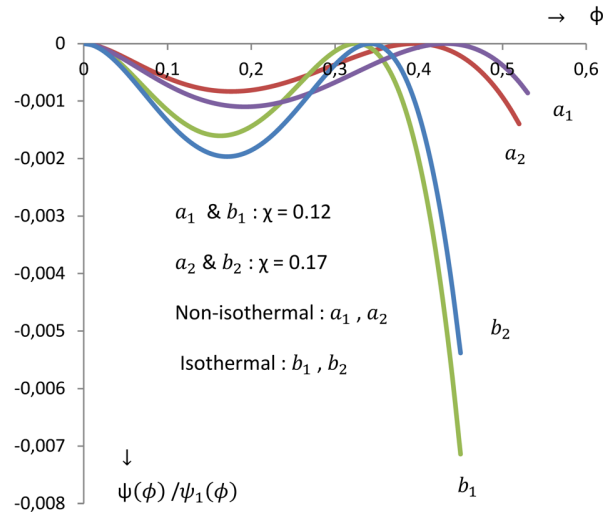


Fig. 1. Comparison of double-layer profiles from Sagdeev potential functions $\psi(\phi)$ and $\psi_1(\phi)$ against ϕ between two-temperature non-isothermal and isothermal electron plasma under a variation of the concentration of positrons (χ) for $V = 1.65, u_{i0} = 0.4, u_{j0} = 0.2, \sigma_i = \frac{1}{100}, \sigma_j = \frac{1}{20}, \sigma_p = 0.41, \beta_1 = 0.02, Q = 1.9, \mu = 0.15, \nu = 0.85, n_{j0} = 0.03, n_{i0} = 0.86, b_l = 0.15, b_h = 0.4$ when $\chi = 0.12$ and 0.17

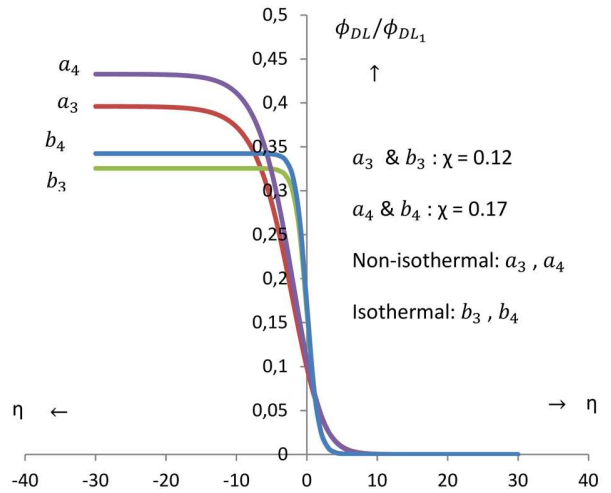


Fig. 2. Comparison of double-layer solution profiles ϕ_{DL} and ϕ_{DL_1} against η between two-temperature non-isothermal and isothermal electron plasma under a variation of the concentration of positrons (χ) for $V = 1.65, u_{i0} = 0.4, u_{j0} = 0.2, \sigma_i = \frac{1}{100}, \sigma_j = \frac{1}{20}, \sigma_p = 0.41, \beta_1 = 0.02, Q = 1.9, \mu = 0.15, \nu = 0.85, n_{j0} = 0.03, n_{i0} = 0.86, b_l = 0.15, b_h = 0.4$ when $\chi = 0.12$ and 0.17

for two-temperature non-isothermal electron plasmas take higher values than that of two-temperature isothermal electron plasmas.

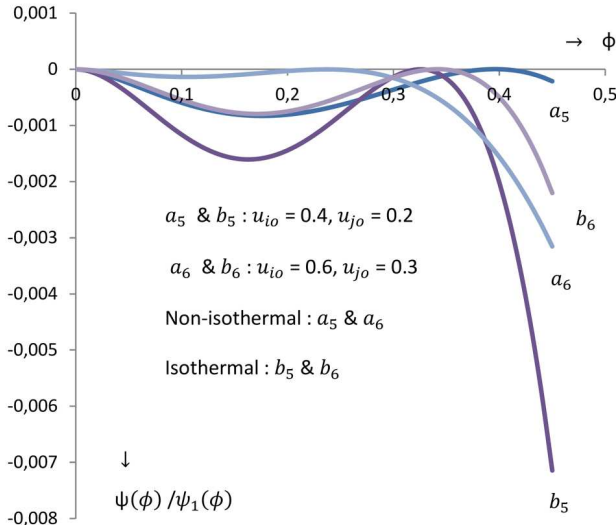


Fig. 3. Comparison of double-layer profiles from Sagdeev potential functions $\psi(\phi)$ and $\psi_1(\phi)$ against ϕ between two-temperature non-isothermal and isothermal electron plasma under variations of the stream velocities of positive (u_{i0}) & negative (u_{j0}) ions for $V = 1.65$, $\chi = 0.12$, $\sigma_i = \frac{1}{100}$, $\sigma_j = \frac{1}{20}$, $\sigma_p = 0.41$, $\beta_1 = 0.02$, $Q = 1.9$, $\mu = 0.15$, $\nu = 0.85$, $n_{j0} = 0.03$, $n_{i0} = 0.86$, $b_l = 0.15$, $b_h = 0.4$ when $u_{i0} = 0.4$, $u_{j0} = 0.2$, $u_{i0} = 0.6$, $u_{j0} = 0.3$

From Figs. 1, 2, the double-layer profiles $\psi_1(\phi)$ and ϕ_{DL1} are not found theoretically for $\chi = 0.08$ when $\sigma_j > \sigma_i$ and $u_{i0} > u_{j0}$ with $n_{j0} = 0.05$, $\beta_1 = 0.02$ in two-temperature isothermal electron plasma, whereas $\psi(\phi)$ and ϕ_{DL} are found for the above-mentioned values of the parameters in two-temperature non-isothermal plasma. But for $\chi = 0.24$ when $\sigma_j < \sigma_i$ and $\beta_1 = 0.02$ with $n_{j0} = 0.03$, $u_{i0} = 0.6$, $u_{j0} = 0.3$, the double-layer profiles $\psi(\phi)$ & $\psi_1(\phi)$ against ϕ and ϕ_{DL} & ϕ_{DL1} against η are both found as compressive double layers in both two-temperature non-isothermal & isothermal electron plasmas whereas the same profiles are not found for $\beta_1 = 0.25$. The amplitudes of the double layers are increasing for increasing values of the concentration of positrons (χ) which shows the effect of positrons.

In our plasma model for Figs. 1 and 2, the small-amplitude double layers are formed and found for $V = 1.65$, $u_{i0} = 0.4$, $u_{j0} = 0.2$, $n_{j0} = 0.03$, $Z = 1$, $\sigma_i = \frac{1}{100}$, $\sigma_j = \frac{1}{20}$, $\sigma_p = 0.41$, $\beta_1 = 0.02$, $Q = 1.9$, $\mu = 0.15$, $\nu = 0.85$, $b_l = 0.15$, $b_h = 0.4$ when χ lies in the range $0 \leq \chi < 1$ and n_{i0} lies in $0.03 < n_{i0} \leq 1.03$ maintaining the charge neutrality condition with physical feasibility of n_{i0} (i.e. $n_{i0} > 0$). It is

also observed and concluded that higher positron concentration ($\chi \geq 1$) increases the electron-to-positron density imbalance which might hinder the formation of small-amplitude double layers. In contrast, $\chi < 1$ provides a better charge distribution, favoring double layers stability. A lower positron concentration, consistent with the quasi-neutrality condition, is required for small-amplitude double layers in our given plasma configuration.

In Fig. 3, the profiles of the double layers from Sagdeev potential functions $\psi(\phi)$ & $\psi_1(\phi)$ against ϕ for small-amplitude double layers between two-temperature non-isothermal & isothermal electron plasmas are compared under the variation of the stream velocities of positive (u_{i0}) and negative (u_{j0}) ions. The Sagdeev potential functions $\psi(\phi)$ for two-temperature non-isothermal electron plasmas are denoted by a_5 for $u_{i0} = 0.4$, $u_{j0} = 0.2$ and a_6 for $u_{i0} = 0.6$, $u_{j0} = 0.3$, whereas the Sagdeev potential functions $\psi_1(\phi)$ for two-temperature isothermal electron plasmas are denoted by b_5 for $u_{i0} = 0.4$, $u_{j0} = 0.2$ and b_6 for $u_{i0} = 0.6$, $u_{j0} = 0.3$. It is observed from this figure that the amplitude for a_5 curve is larger than the amplitude for b_5 curve, when $u_{i0} = 0.4$, $u_{j0} = 0.2$, whereas the amplitude for a_6 curve is smaller than the amplitude for b_6 curve, when $u_{i0} = 0.6$, $u_{j0} = 0.3$. Thus, it is concluded that if stream velocities are increasing, the amplitude of two-temperature isothermal electron plasma is larger than the amplitude of two-temperature non-isothermal electron plasma.

Fig. 4 shows the profiles of the double-layer solutions ϕ_{DL} and ϕ_{DL1} against η for two-temperature non-isothermal & isothermal electron plasmas under variations of the stream velocities of positive (u_{i0}) & negative (u_{j0}) ions. The double layer solutions ϕ_{DL} for two-temperature non-isothermal electron plasmas are denoted by a_7 for $u_{i0} = 0.4$, $u_{j0} = 0.2$ and a_8 for $u_{i0} = 0.6$, $u_{j0} = 0.3$ whereas the double-layer solutions ϕ_{DL1} for two-temperature isothermal electron plasmas are denoted by b_7 for $u_{i0} = 0.4$, $u_{j0} = 0.2$ and b_8 for $u_{i0} = 0.6$, $u_{j0} = 0.3$. It is interesting to note that for larger value of the stream velocity $u_{i0} = 0.6$, $u_{j0} = 0.3$ in our model, the corresponding curve a_8 takes lower values than the curve a_7 for its stream velocity $u_{i0} = 0.4$, $u_{j0} = 0.2$ in our model. Again, the curve a_7 takes larger value than b_7 for $u_{i0} = 0.4$, $u_{j0} = 0.2$ whereas the curve a_8 takes smaller value than the curve b_8 for $u_{i0} = 0.6$, $u_{j0} = 0.3$. For stream

velocity $u_{i0} = 0.4$, $u_{j0} = 0.2$, the curve a_7 takes higher value than the curve b_7 whereas for stream velocity $u_{i0} = 0.6$, $u_{j0} = 0.3$, the curve a_8 possesses lower value than the curve b_8 .

In non-streaming motion of positive and negative ions ($u_{i0} = 0$, $u_{j0} = 0$) with $\chi = 0.12$, $\sigma_i = \frac{1}{100}$, $\sigma_j = \frac{1}{20}$, $n_{j0} = 0.03$, $\beta_1 = 0.02$ and $V = 1.65$, the double layers are formed only for two-temperature non-isothermal electron plasmas but it is impossible to form double layer profiles for two-temperature isothermal electron plasma under the variation of the same plasma parameters with $u_{i0} = 0$, $u_{j0} = 0$ which is an important situation in our model.

From Figs. 3 and 4, it is found that the stream velocities of positive and negative ions play a crucial role in determining the characteristics of ion-acoustic double layers. Higher ion velocities generally lead to weaker, broader and less stable double layers, as ions are less likely to accumulate near the potential well. In contrast, lower ion velocities allow for better accumulation of ions in the double-layer region, leading to stronger, narrower and more stable structures. The balance between positive and negative ion velocities is important for maintaining the symmetry and stability of the double layer, and any significant velocity imbalance can destabilize the structure or lead to more complex plasma dynamics.

In Fig. 5, the profiles of the double layers from Sagdeev potential functions $\psi(\phi)$ & $\psi_1(\phi)$ against ϕ for small amplitude double layers are compared between two-temperature non-isothermal & isothermal electron plasmas under the variation of the temperatures of positive (σ_i) and negative (σ_j) ions. The Sagdeev potential functions $\psi(\phi)$ for two-temperature non-isothermal electron plasmas are denoted by a_9 for $\sigma_i = 1/100$, $\sigma_j = 1/20$ and a_{10} for $\sigma_i = 1/30$, $\sigma_j = 1/100$, whereas the Sagdeev potential functions $\psi_1(\phi)$ for two-temperature isothermal electron plasmas are denoted by b_9 for $\sigma_i = 1/100$, $\sigma_j = 1/20$ and b_{10} for $\sigma_i = 1/30$, $\sigma_j = 1/100$. The amplitude for the curve a_9 is greater than the amplitude of the curve a_{10} in two-temperature non-isothermal electron plasma and also the depth of the well for the curve a_9 is larger than the curve a_{10} . Again the amplitude of the curve b_9 is smaller than the amplitude of the curve b_{10} , but the well depth of the curve b_{10} is higher than that of b_9 . It is seen clearly from this figure that the amplitude of the curve a_9 is larger than the amplitude of the curve

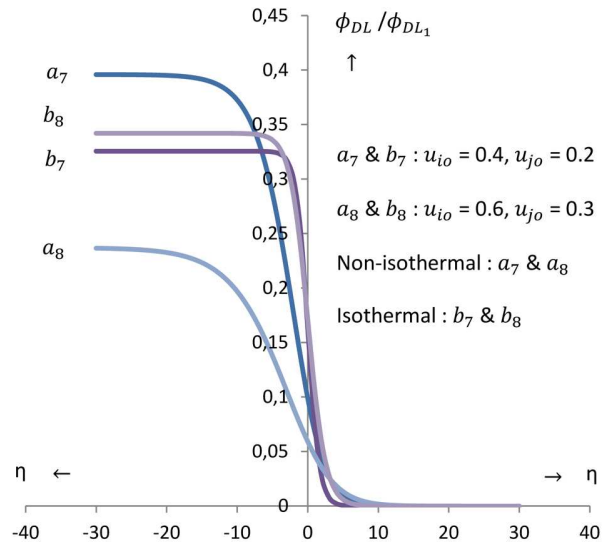


Fig. 4. Comparison of double-layer solution profiles ϕ_{DL} and ϕ_{DL1} against η between two-temperature non-isothermal and isothermal electron plasma under variations of the stream velocities of positive (u_{i0}) & negative (u_{j0}) ions for $V = 1.65$, $\chi = 0.12$, $\sigma_i = \frac{1}{100}$, $\sigma_j = \frac{1}{20}$, $\sigma_p = 0.41$, $\beta_1 = 0.02$, $Q = 1.9$, $\mu = 0.15$, $\nu = 0.85$, $n_{j0} = 0.03$, $n_{i0} = 0.86$, $b_l = 0.15$, $b_h = 0.4$ when $u_{i0} = 0.4$, $u_{j0} = 0.2$, $u_{i0} = 0.6$, $u_{j0} = 0.3$

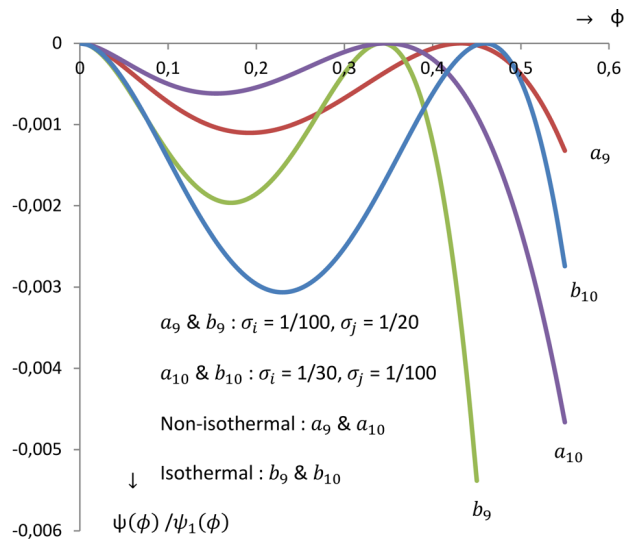


Fig. 5. Comparison of double-layer profiles from Sagdeev potential functions $\psi(\phi)$ and $\psi_1(\phi)$ against ϕ between two-temperature non-isothermal and isothermal electron plasma under variations of the temperatures of positive (σ_i) & negative (σ_j) ions for $V = 1.65$, $\chi = 0.17$, $\sigma_p = 0.41$, $\beta_1 = 0.02$, $Q = 1.9$, $\mu = 0.15$, $\nu = 0.85$, $n_{j0} = 0.03$, $n_{i0} = 0.86$, $b_l = 0.15$, $b_h = 0.4$, $u_{i0} = 0.4$, $u_{j0} = 0.2$ when $\sigma_i = \frac{1}{100}$, $\sigma_j = \frac{1}{20}$, $\sigma_i = \frac{1}{30}$, $\sigma_j = \frac{1}{100}$

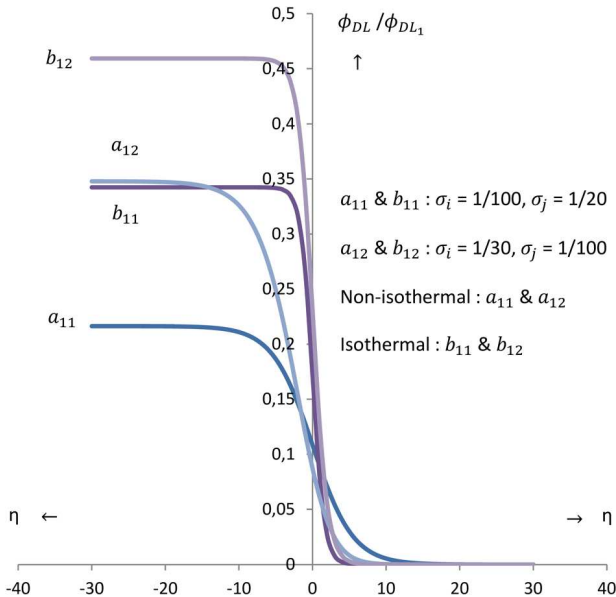


Fig. 6. Comparison of double-layer solution profiles ϕ_{DL} and ϕ_{DL_1} against η between two-temperature non-isothermal and isothermal electron plasma under variations of the temperatures of positive (σ_i) & negative (σ_j) ions for $V = 1.65$, $\chi = 0.17$, $\sigma_p = 0.41$, $\beta_1 = 0.02$, $Q = 1.9$, $\mu = 0.15$, $\nu = 0.85$, $n_{j0} = 0.03$, $n_{i0} = 0.86$, $b_l = 0.15$, $b_h = 0.4$, $u_{i0} = 0.4$, $u_{j0} = 0.2$, when $\sigma_i = \frac{1}{100}$, $\sigma_j = \frac{1}{20}$; $\sigma_i = \frac{1}{30}$, $\sigma_j = \frac{1}{100}$

b_9 , when $\sigma_i = 1/100$, $\sigma_j = 1/20$ and similarly the amplitude of the curve a_{10} is smaller than that of the curve b_{10} , when $\sigma_i = 1/30$, $\sigma_j = 1/100$.

Figure 6 shows the profiles of the double-layer solutions ϕ_{DL} and ϕ_{DL_1} against η for two-temperature non-isothermal & isothermal electron plasmas under variations of the temperatures of positive (σ_i) and negative (σ_j) ions. The double layer solutions ϕ_{DL} for two-temperature non-isothermal electron plasmas are denoted by a_{11} for $\sigma_i = 1/100$, $\sigma_j = 1/20$ and a_{12} for $\sigma_i = 1/30$, $\sigma_j = 1/100$, whereas the double-layer solutions ϕ_{DL_1} for two-temperature isothermal electron plasmas are denoted by b_{11} for $\sigma_i = 1/100$, $\sigma_j = 1/20$ and b_{12} for $\sigma_i = 1/30$, $\sigma_j = 1/100$. For $\sigma_i = 1/30$, $\sigma_j = 1/100$, the curve a_{12} takes larger value than the curve a_{11} for $\sigma_i = 1/100$, $\sigma_j = 1/20$ whereas the curve b_{12} for $\sigma_i = 1/30$, $\sigma_j = 1/100$ also takes higher values than that of the curve b_{11} for $\sigma_i = 1/100$, $\sigma_j = 1/20$. Again the curve a_{11} takes smaller value than that of the curve b_{11} , when $\sigma_i = 1/100$, $\sigma_j = 1/20$ and similarly the curve a_{12} takes smaller value than that of the curve b_{12} for $\sigma_i = 1/30$, $\sigma_j = 1/100$.

The double-layer structures in Fig. 6 represent the potential variation across the double layers. The asymmetric shape of this double layers mainly arises due to the differences in temperatures. Actually, the potential starts at the baseline, rises to a peak and returns to the baseline. In the analysis of this figure, the differences in the curves are, thus, primarily driven by the electron energy distribution, thermal effects of ions and positrons, and the relative densities of the plasma species. These parameters dictate the balance of forces in the plasma and the resulting structure of the ion-acoustic double layers.

In Figs. 5 & 6, we are considering the following two situations on the basis of the temperatures of positive (σ_i) and negative (σ_j) ions as $\sigma_j > \sigma_i$ and $\sigma_j < \sigma_i$. In both cases for two-temperature non-isothermal and isothermal electron plasmas, double-layer profiles from Sagdeev potential functions and double-layer solutions are obtained for $u_{i0} = 0.4$, $u_{j0} = 0.2$, $\chi = 0.17$ with $\beta_1 = 0.02$.

Again, from Figs. 5 and 6, it can be concluded that the asymmetric shape of double layers arises due to the differences in temperatures and densities of the concerned plasma species. The temperatures of both positive and negative ions significantly affect the formation, structure and behavior of ion-acoustic double layers. Hotter ions lead to reducing the strength of the double layer, making it weaker and broader, while colder ions tend to reinforcing the structure, resulting in a stronger and narrower potential barrier. The temperature imbalance between the two types of ions can lead to more complex dynamics, affecting the overall stability and characteristics of ion-acoustic double layers in plasmas.

In Fig. 7, the profiles of the double layers from Sagdeev potential functions $\psi(\phi)$ & $\psi_1(\phi)$ against ϕ for small-amplitude double layers are compared between two-temperature non-isothermal & isothermal electron plasmas under variations of the concentrations of negative (n_{j0}) ions. The Sagdeev potential functions $\psi(\phi)$ for two-temperature non-isothermal electron plasmas are denoted by a_{13} for $n_{j0} = 0.01$ and a_{14} for $n_{j0} = 0.03$ whereas the Sagdeev potential functions $\psi_1(\phi)$ for two-temperature isothermal electron plasmas are denoted by b_{13} for $n_{j0} = 0.01$ and b_{14} for $n_{j0} = 0.03$. It is interesting to observe that, for $n_{j0} = 0.01$, the amplitude of the curve a_{13} is less than the amplitude of the curve b_{13} , whereas, for $n_{j0} = 0.03$, the amplitude of the curve a_{14} is greater

than that of the curve b_{14} . Moreover, the amplitude of the curve a_{14} at $n_{j0} = 0.03$ is greater than the amplitude of the curve a_{13} for $n_{j0} = 0.01$ whereas the amplitude of the curve b_{13} for $n_{j0} = 0.01$ is higher than the amplitude of the curve b_{14} for $n_{j0} = 0.03$.

Fig. 8 shows the profiles of the double-layer solutions ϕ_{DL} and ϕ_{DL1} against η for two-temperature non-isothermal & isothermal electron plasmas under variations of the concentrations of negative (n_{j0}) ions. The double layer solutions ϕ_{DL} for two-temperature non-isothermal electron plasmas are denoted by a_{15} for $n_{j0} = 0.01$ and a_{16} for $n_{j0} = 0.03$ whereas the double layer solutions ϕ_{DL1} for two-temperature isothermal electron plasmas are denoted by b_{15} for $n_{j0} = 0.01$ and b_{16} for $n_{j0} = 0.03$. For $n_{j0} = 0.03$, the curve a_{16} takes larger value than the curve a_{15} for $n_{j0} = 0.01$ whereas the curve b_{15} for $n_{j0} = 0.01$ also takes higher values than that of the curve b_{16} for $n_{j0} = 0.03$. Again the curve a_{15} takes smaller value than that of the curve b_{15} when $n_{j0} = 0.01$ and similarly the curve a_{16} takes larger value than that of the curve b_{16} for $n_{j0} = 0.03$.

Moreover, it is found that the profiles of double layers exist only in two-temperature non-isothermal electron plasma for $n_{j0} = 0.05$ when $\chi = 0.12$, $u_{i0} = 0.4$, $u_{j0} = 0.2$, $\sigma_i = \frac{1}{100}$, $\sigma_j = \frac{1}{20}$, $\beta_1 = 0.02$ and $V = 1.65$ but the same profiles do not exist and found for the same parameters in two-temperature isothermal electron plasma which is an important situation.

From Figs. 7 and 8, it is found that the concentration of negative ions plays a key role in shaping the characteristics of ion-acoustic double layers. Higher concentration of negative ions generally lead to stronger, more stable double layers with deeper potential drops and narrower widths. They help one to maintain the charge neutrality and stabilize the electrostatic structure of the double layer. However, if the concentration of negative ions becomes too high, it may destabilize the double layer or prevent its formation. The overall effect depends on the balance between positive and negative ion densities and their temperatures, as well as the interplay between ions and electrons in the plasma.

4. Comparative Studies

Our next task is to compare the nature and shape of the profiles of the double layers from the Sagdeev potential functions $\psi(\phi)$ & $\psi_1(\phi)$ against ϕ and dou-

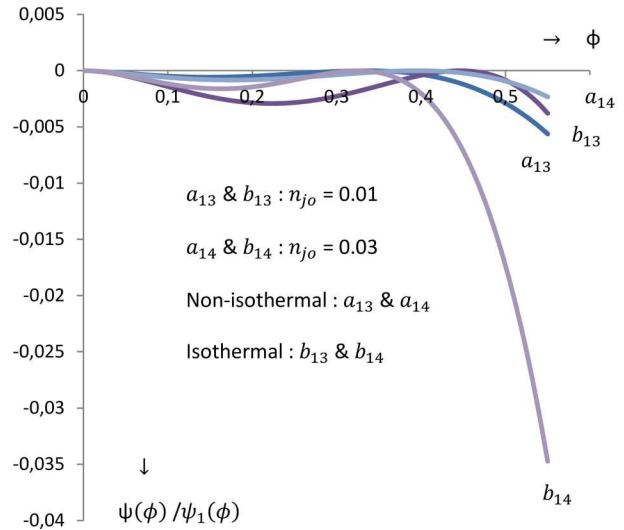


Fig. 7. Comparison of double-layer profiles from Sagdeev potential functions $\psi(\phi)$ and $\psi_1(\phi)$ against ϕ between two-temperature non-isothermal and isothermal electron plasma under variations of the concentrations of negative ions (n_{j0}) for $V = 1.65$, $\chi = 0.12$, $\sigma_p = 0.41$, $\beta_1 = 0.02$, $Q = 1.9$, $\mu = 0.15$, $\nu = 0.85$, $n_{i0} = 0.89, 0.91$, $b_l = 0.15$, $b_h = 0.4$, $u_{i0} = 0.4$, $u_{j0} = 0.2$, $\sigma_i = \frac{1}{100}$, $\sigma_j = \frac{1}{20}$ when $n_{j0} = 0.01, 0.03$

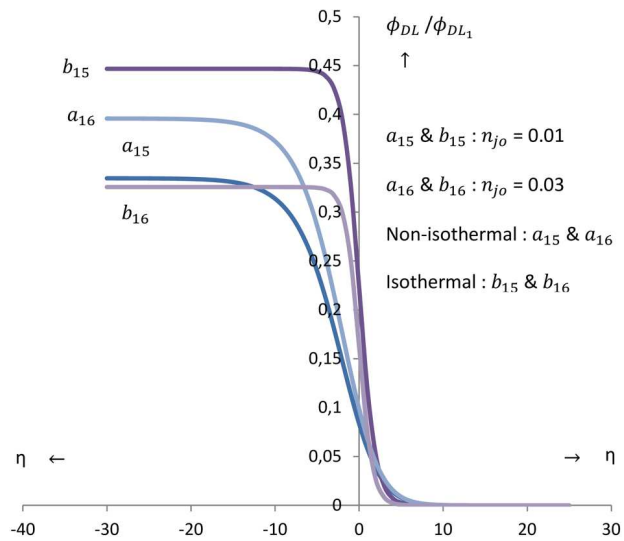


Fig. 8. Comparison of double-layer solution profiles ϕ_{DL} and ϕ_{DL1} against η between two-temperature non-isothermal and isothermal electron plasma under variations of the concentrations of negative ions (n_{j0}) for $V = 1.65$, $\chi = 0.12$, $\sigma_p = 0.41$, $\beta_1 = 0.02$, $Q = 1.9$, $\mu = 0.15$, $\nu = 0.85$, $n_{i0} = 0.89, 0.91$, $b_l = 0.15$, $b_h = 0.4$, $u_{i0} = 0.4$, $u_{j0} = 0.2$, $\sigma_i = \frac{1}{100}$, $\sigma_j = \frac{1}{20}$, when $n_{j0} = 0.01, 0.03$

ble layer solutions ϕ_{DL} & ϕ_{DL_1} against η for small-amplitude double layers between two-temperature non-isothermal and isothermal electron plasmas under variations of the different values of the positron densities (χ), stream velocities of positive (u_{i0}) and negative (u_{j0}) ions, temperatures of positive (σ_i) and negative (σ_j) ions and the concentrations of negative ions (n_{j0}) which are shown clearly under the graphical approach by the respective Figs. 1 to 8. In $\psi(\phi)$ and ϕ_{DL} for two-temperature non-isothermal electron plasmas, the values of the expression for G_3 and ϕ_m are positive, whereas, in $\psi_1(\phi)$ and ϕ_{DL_1} for two-temperature isothermal electron plasmas, the values of G_5 and ϕ_{m_1} are also positive in order to obtain the profiles of the compressive double layers. The double-layer points [ϕ_m and ϕ_{m_1} i.e. at which double layer occurs] for this compressive double layers are also varied and are shown by the tangency condition [$\frac{\partial\psi}{\partial\phi} = 0$ and $\frac{\partial\psi_1}{\partial\phi} = 0$] in both two-temperature non-isothermal and isothermal electron plasmas. Again, it is found by observation, that, after a certain maximum value of soliton velocity V , no solitary waves are found nearer to V , and then there may be a possibility of the formation of a double layer. When the velocity V crosses the soliton maximum velocity limit, then our present plasma model shows the compressive double layers at some specific values of V larger than the maximum soliton velocity, and that specific value of V must satisfy the required double-layer conditions under variations of different plasma parameters consistent with the quasi-neutrality condition for both two-temperature non-isothermal and two-temperature isothermal electron plasmas. Indeed, in most cases, the values of V at which double layers occur in two-temperature non-isothermal electron and in two-temperature isothermal electron plasmas are certainly different due to the differences in the temperature profiles and electric potentials in the double layers, but, in some simplified or idealized models for comparison of small-amplitude double layer profiles, we take such specific values of V or the same values of V at which double layer occurs in both two-temperature non-isothermal and isothermal electron plasmas and satisfy the necessary boundary conditions of double layers. In our plasma model, the small-amplitude double layers are formed and found for $V = 1.65$, $u_{i0} = 0.4$, $u_{j0} = 0.2$, $n_{j0} = 0.03$, $Z = 1$, $\sigma_i = \frac{1}{100}$, $\sigma_j = \frac{1}{20}$, $\sigma_p = 0.41$, $\beta_1 = 0.02$, $Q = 1.9$, $\mu = 0.15$, $\nu = 0.85$, $b_l = 0.15$, $b_h = 0.4$

when χ lies in the interval $0 \leq \chi < 1$, and n_{i0} lies in $0.03 < n_{i0} \leq 1.03$ maintaining the charge neutrality condition with physical feasibility of n_{i0} (i.e., $n_{i0} > 0$). It is also observed and concluded that higher positron concentration ($\chi \geq 1$) increases the electron-to-positron density imbalance which might hinder the formation of small amplitude double layers. In contrast, $\chi < 1$ provides a better charge distribution, favoring the double layer stability. A lower positron concentration, consistent with the quasi-neutrality condition, is required for small-amplitude double layers in our given plasma configuration.

On the other hand, the comparison between two models for small amplitude double layers may be described by the general approach. The general approach involves developing a set of equations for both isothermal and non-isothermal plasmas, linearizing these equations, solving for the dispersion relation, and deriving the conditions under which double layers are formed. The key differences between the isothermal and non-isothermal cases lie in the temperature profiles of the species, which influence the charge distribution, potential profile, and the dynamics of the double layer.

The comparisons of double layers between two-temperature non-isothermal and isothermal electron plasmas are largely theoretical. Validation through experiments or simulations is limited. This theoretical comparisons between two-temperature non-isothermal and isothermal electron plasmas containing warm positive ions, warm negative ions, and warm positrons are consistent with simulations, but only partially validated by experiments. Simulations provide robust support for these theories, confirming the predicted differences in ion-acoustic double-layer properties. Experimental work in this area is ongoing, but faces significant technical challenges.

5. Conclusions

We have investigated the double-layer profiles from Sagdeev potential functions $\psi(\phi)$ & $\psi_1(\phi)$ against ϕ and double-layer solutions ϕ_{DL} and ϕ_{DL_1} against η for the comparative analysis between two-temperature non-isothermal [$\psi(\phi), \phi_{DL}$] & isothermal [$\psi_1(\phi), \phi_{DL_1}$] electron plasmas under variations of some plasma parameters. The graphical representations of the Sagdeev potential functions $\psi(\phi)$ and $\psi_1(\phi)$ against ϕ for small-amplitude double layers

have been observed by many Physicists under variations of different concerned plasma parameters in two-temperature non-isothermal and isothermal electron plasmas. But the comparative studies of the double layers from Sagdeev potential functions and double-layer solutions for both two-temperature non-isothermal and isothermal electron plasmas are not yet found in any plasma paper and are, therefore, supposed to be a new findings. From this comparison, anyone can get an idea about their amplitudes, widths, depths of the Sagdeev potential well, energy level, and behaviour under variations of the concerned parameters like concentrations of positrons (χ), stream velocities of positive (u_{i0}) and negative (u_{j0}) ions, temperatures of positive (σ_i) and negative (σ_j) ions and concentrations of negative ions (n_{j0}). In our model plasma, it is worth to note that the compressive double layer occurs at $V = V_{dl} = 1.65$ which is the upper limit to the soliton velocity range with different amplitudes ($\phi = \phi_{dl} = \phi_m$ or ϕ_{m1}) in two-temperature non-isothermal and isothermal electron plasmas for some variation of the values of the concerned plasma parameters. Here, V_{dl} and ϕ_{dl} are some particular values of the soliton velocity V and the electrostatic potential ϕ at which double layer occurs. The concerned limiting electrostatic potential $\phi_{lp} = \phi = \frac{1}{2} \left(V - u_{i0} - \sqrt{\frac{3\sigma_i}{n_{i0}}} \right)^2$ for that compressive double layer, is found in such a way that the condition $\phi_{dl} < \phi_{lp}$ is always satisfied, where the density of the positive ion (n_i) is real-valued, which shows the existence domain of the compressible double layers. But, after crossing the limiting electrostatic potential (ϕ_{lp}), the positive ion density (n_i) will be complex-valued everywhere for which no double layers will be observed there. The concentration of positrons (χ) is also an interesting parameter for the formation of double layers in the given plasma configuration. Theoretical observations show that the small-amplitude double layers are formed for $0 \leq \chi < 1$ consistent with the quasi-neutrality condition in our model, but no double layers are observed, when $\chi > 1$. In this context, it is further mentioned that double layers are often associated with strong electric fields and can accelerate charged particles to high energies. It can also contribute to plasma confinement by forming boundaries between different plasma regions. This paper likely focuses on studying the characteristics of double lay-

ers and explores the differences in double-layer structures in plasma environments with distinct temperature profiles. The behavior of plasmas under different temperature conditions is crucial for understanding the structures in the Earth's magnetosphere or the solar wind. This study can help us to explain how double layers are formed in these environments and influence phenomena like auroras and solar flares. Again, double layers in non-isothermal and isothermal conditions could offer insights into the behavior of astrophysical plasmas around stars, in interstellar space or in accretion disks around black holes. Actually, the applications of this research paper are diverse, ranging from improving our understanding of space and astrophysical plasmas to enhancing fusion technology and industrial processes. The comparative analysis of double-layer profiles under different temperature conditions provides valuable insights that can be applied across various domains in plasma physics.

The future plan of the present author is to find the comparative analysis of large-amplitude ion-acoustic double layers for two-temperature non-isothermal electrons in magnetized and in unmagnetized plasmas containing warm negative ions and warm positive ions.

The present author is very much grateful to the referees for their valuable guidelines in the improvement of this work and would like to thank Dr. S.N. Paul for his valuable suggestions in the preparation of this paper in its present form.

1. R.Z. Sagdeev. *Reviews of Plasma Physics*. Edited by M.A. Leontovich (Consultants Bureau, 1966).
2. C.P. Olivier, S.K. Maharaj, R. Bharuthram. Ion-acoustic solitons, double layers and super solitons in a plasma with two ion and two electron species. *Phys. Plasmas* **22**, 082312 (2015).
3. G.S. Lakhina, S.V. Singh, A.P. Kakad, F. Verheest, R. Bharuthram. Study of non-linear ion and electron-acoustic waves in multicomponent space plasmas. *Non-Linear Processes in Geophysics* **15**, 903 (2008).
4. O.R. Rufai, R. Bharuthram, S.V. Singh, G.S. Lakhina. Low frequency solitons and double layers in a magnetized plasma with two-temperature electrons. *Phys. Plasmas* **19**, 122308 (2012).
5. A. Paul, A. Bandyopadhyay. Ion-acoustic solitons, double layers and super solitons in a collisionless unmagnetized plasma consisting of nonthermal electrons and isothermal positrons. *Indian J. Physics* **92** (9), 1187 (2018).
6. S. Dalui, S. Sardar, A. Bandyopadhyay. Arbitrary amplitude ion-acoustic solitons, double layers and super soli-

- tons in a collisionless magnetized plasma consisting of non-thermal and isothermal electrons. *Zeitschrift fur Naturforschung A* **76**, 455 (2021).
7. S.G. Tagare. Ion-acoustic solitons and double layers in a two-electron temperature plasma with hot isothermal electrons and cold ions. *Phys. Plasmas* **7**, 883 (2000).
 8. P. Carlqvist. On the acceleration of energetic cosmic particles by electrostatic double layers. *IEEE Trans. Plasma Sci.* **14** (6), 794 (1986).
 9. D.E. Baldwin, B.G. Logan. Improved Tandem mirror fusion reactor. *Phys. Rev. Lett.* **43**, 1318 (1979).
 10. K. Saeki, S. Iizuka, N. Sato. Ion heating due to double layer disruption in a plasma. *Phys. Rev. Lett.* **45**, 1853 (1980).
 11. M. Temerin, K. Cerny, W. Lotko, F.S. Mozer. Observations of double layers and solitary waves in the auroral plasma. *Phys. Rev. Lett.* **48**, 1175 (1982).
 12. R. Bostrom, G. Gustafsson, B. Holback, G. Holmgren, H. Koskinen, P. Kintner. Characteristics of solitary waves and weak double layers in the magnetospheric plasma. *Phys. Rev. Lett.* **61**, 82 (1988).
 13. R.L. Merlino, J.J. Loomis. Double layers in a plasma with negative ions. *Phys. Fluids B* **2**, 2865 (1990).
 14. A.Y. Wong, D.L. Mamas, D. Arnush. Negative ion plasmas. *Phys. Fluids* **18**, 1489 (1975).
 15. N. Sato. Production of negative ion plasmas in a Q machine. *Plasma Sour. Sci. Technol.* **3** (3), 395 (1994).
 16. M.K. Mishra, A.K. Arora, R.S. Chhabra. Ion-acoustic compressive and rarefactive double layers in a warm multicomponent plasma with negative ions. *Phys. Rev. E* **66**, 046402 (2002).
 17. K.S. Goswami, S. Bujarbarua. Theory of weak ion-acoustic double layers. *Phys. Lett. A* **108**, 149 (1985).
 18. T.S. Gill, P. Bala, H. Kaur, N.S. Saini, S. Bansal, J. Kaur. Ion-acoustic solitons and double layers in a plasma consisting of positive and negative ions with non-thermal electrons. *Euro. Phys. J. D* **31**, 91 (2004).
 19. S. Chattopadhyay, S.N. Paul. Compressive and rarefactive solitary waves in plasma with cold drifting positive and negative ions. *The African Rev. Phys.* **7** (0033), 289 (2012).
 20. S. Chattopadhyay. Compressive solitons and double layers in non-isothermal plasma. *Brazilian J. Phys.* **52**, 4 (2022).
 21. S. Chattopadhyay. Higher order solitons and double layers in non-isothermal plasma. *Brazilian J. Phys.* **53**, 6 (2023).
 22. M.K. Mishra, R.S. Tiwari, J.K. Chawla. Ion-acoustic solitons in negative ion plasma with two-electron temperature distributions. *Phys. Plasmas* **19**, 062303 (2012).
 23. K. Kumar, M.K. Mishra. Large amplitude ion-acoustic solitons in warm negative ion plasmas with superthermal electrons. *AIP Adv.* **7**, 115114 (2017).
 24. S. Chattopadhyay. Existence of small – amplitude double layers in two-temperature non-isothermal plasma. *Ukr. J. Phys.* **68** (12), 795 (2023).
 25. K.Y. Kim. Theory of weak shock-like structures. *Phys. Lett. A* **136** (1–2), 63 (1989).
 26. J.M. Han, K.Y. Kim. Weak non-monotonic double layers and shock-like structures in multispecies plasma. *Plasma Phys. Control. Fusion* **36** (7), 1141 (1994).
 27. Tae Han Kim, Kwang Youl Kim. Ion acoustic monotonic double layer in a weak relativistic plasma. *J. Korean Phys. Soc.* **42** (3), 363 (2003).
 28. T.H. Kim, K.Y. Kim. Modified K-dV theory of non-monotonic double layer in a weak relativistic plasma. *Phys. Letts. A* **286** (2–3), 180 (2001).
 29. H. Schamel. Analytic BGK modes and their modulational instability. *J. Plasma Phys.* **13**, 139 (1975).
 30. G. Joyce, R.F. Hubbard. Numerical simulation of plasma double layers. *J. Plasma Phys.* **20** (3), 391 (1978).
 31. K.D. Baker, N. Singh, L.P. Block, R. Kist, W. Kampa, H. Thiemann. Studies of strong laboratory double layers and comparison with computer simulation. *J. Plasma Phys.* **26** (1), 1 (1981).
 32. T. Sato, H. Okuda. Numerical simulations on ion-acoustic double layers. *J. Geophys. Res.: Space Phys.* **86** (A5), 3357 (1981).
 33. N. Hershkowitz. Review of recent laboratory double layer experiments. *Space Sci. Rev.* **41**, 351 (1985).
 34. J.L. Ferreira, G.O. Ludwig, A. Montes. Experimental investigation of ion-acoustic double layers in the electron flow across multidipole magnetic fields. *Plasma Phys. Controlled Fusion* **33** (4), 297 (1991).
 35. C. Charles. A review of recent laboratory double layer experiments. *Plasma Sources Science and Technology* **16** (4), (2007).

Received 22.09.24

C. Чаттопадхяй

ПОРІВНЯЛЬНИЙ АНАЛІЗ ПРОФІЛЕЙ
ПОДВІЙНИХ ШАРІВ МІЖ ДВОТЕМПЕРАТУРНОЮ
НЕІЗОТЕРМІЧНОЮ ТА ІЗОТЕРМІЧНОЮ
ЕЛЕКТРОННОЮ ПЛАЗМОЮ

Розглядаються подвійні шари між двотемпературною неізо-термічною та ізоетермічною електронною плазмою. Аналіз показав залежності двошарових структур від параметрів потенціалу Сагдєєва і профілів температур. Отримані результати можуть бути застосовані в різних розділах теорії плазми.

Ключові слова: псевдопотенціал Сагдєєва, подвійні шари, двотемпературні неізоетермічні та ізоетермічні електрони, швидкості потоків, температури позитивно і негативно заряджених іонів, концентрації позитронів і негативно заряджених іонів.